Environmental Engineering and Management Journal November/December 2008, Vol.7, No.6, 701-706
http://omicron.ch.tuiasi.ro/EEMJ/

"Gheorghe Asachi" Technical University of Iasi, Romania

EFFECT OF VANADIUM REPLACEMENT BY ZIRCONIUM ON THE ELECTROCHEMICAL BEHAVIOR OF Ti6Al4V ALLOY IN RINGER´S SOLUTION

Daniel Mareci[1*], Daniel Sutiman[1], Adrian Cailean[1], Igor Crețescu[2]

[1]"Gheorghe Asachi" Technical University of Iasi, Faculty of Chemical Engineering and Environmental Protection, Department of Chemical Engineering, [2]Department of Environmental Engineering and Management, 71 Mangeron Blvd., 700050, Iaşi, Romania

Abstract

The electrochemical behaviour of Ti6Al4V and Ti6Al4Zr alloys has been evaluated in Ringer's solution at 25^0C. The effect of the substitution of vanadium in Ti6Al4V alloy has been specifically addressed. The evaluation of the corrosion resistance was carried out through the analysis of the open circuit potential variation with time, potentiodynamic polarization curves, and electrochemical impedance spectroscopy (EIS) tests. Very low current densities were obtained (order of nA/cm^2) from the polarization curves and EIS, indicating a typical passive behaviour for both investigated alloys. The EIS results exhibited capacitive behaviour (large corrosion resistance) with phase angle close to -80^0 and high impedance values (order of 10^5 Ω cm^2) at low and medium frequencies, which are indicative of the formation of a highly stable film on these alloys in Ringer's solution. In conclusion, the electrochemical behaviour of Ti6Al4V is not affected on substituting vanadium with zirconium.

Key words: current corrosion, impedance, polarization, Titanium alloys

1. Introduction

Commercial titanium and titanium alloys are used on a large scale in medical applications as implants to restore lost functions or replace organs functioning below acceptable levels, due to their advantages as compared with other similar materials: chemical inertia, low densities, toxicity absence and higher biocompatibility (Assis et al., 2006; Eriksson et al., 2007; Kim et al., 2007; Mantani and Tajima, 2006; Newman et al., 1988; Taddei et al., 2004).

The physical metallurgy of titanium shows that it undergoes an allotropic transformation at about 885°C, changing from a close-packed hexagonal (c.p.h.) crystal structure (i.e. alpha phase) to a body-centred cubic (b.c.c.) crystal structure (i.e. beta phase). Alloying elements are known to either lower or raise the transformation temperature. Depending on their microstructure, titanium alloys fall into five categories: alpha, near-alpha, alpha-beta, near-beta or beta. Each of these denotes the general type of microstructure present after heat treatment and processing (Boyer and Gall, 1985; Collings, 1984; Donachie, 1988). Substitutional alloying elements play an important role in controlling the microstructure and properties of titanium alloys.

Vanadium and niobium are beta amorphous with b.c.c. titanium (Boyer and Gall, 1985). Zirconium is one that is unique in that it is isomorphous with both the alpha and beta phases of titanium (Donachie, 1988). Beta isomorphous elements are preferred since they do not form intermetallic compounds. The aluminium continues to fulfil its role as a useful alpha phase stabilizer, and thus, maintain the improved mechanical properties over pure titanium.

Ever since the pioneer metal alloys have been use as biomaterials, lack of biocompatibility has been extensively reported and research on improved materials with appropriate mechanical behaviour and adequate biocompatibility was developed. The Ti6Al4V alloy was the first titanium alloy registered as implant material in the ASTM standards (F-136-84). Further studies have indicated that vanadium,

* Author to whom all correspondence should be addressed: danmareci@yahoo.com

used to stabilize the beta-phase, produces harmful oxides for the human body (Hallab et al., 2005; Okazaki et al., 1998). The toxicity of vanadium pushed forward the search for materials to replace Ti6Al4V.

Ti, Nb, Zr, Pd and Ta are low cytotoxic elements (Okazaki et al., 1998). The Ti6Al7Nb alloy was developed using the alloying element niobium to replace vanadium in the Ti6Al4V alloy. It has been suggested by Khan et al., (1996) that Ti6Al7Nb alloy can be a better alternative to Ti6Al4V alloy because of its corrosion resistance and resistance to loss of mechanical properties with changes in pH in simulated body fluid environment.

Electrochemical behaviour of the implant materials in physiological medium is necessary to access the nature of the passive film formed and its role in biocompatibility.

Electrochemical behavior of the pure titanium and several (alpha + beta) titanium alloys in Ringer's solution was the subject of a number of prior investigations (Gonzalez and Mirza Rosca, 1999; Kuphasuk et al., 2001; Mirza Rosca et al., 2008; Popa et al., 2004).

In the present study, the electrochemical and corrosion behaviour of Ti6Al4V alloy has been compared with that of Ti6Al4Zr alloy in which vanadium was replaced with zirconium.

2. Materials and methods

2.1. Materials and sample preparation

The Ti6Al4V and Ti6Al4Zr alloys used in present investigation were acquired in form of a road from National Institute of Research & Development for Non-ferrous and Rare Metals, Bucharest, Romania. The both alloys were submitted to a semi-quantitative chemical analysis by plasma optical emission spectrometry technique and its results are given in Table 1.

The testing medium was an aerated Ringer's solution whose composition is: NaCl – 8.6 g/L, KCl – 0.3 g/L, $CaCl_2$ – 0.48 g/L.

The pH was measured with a multiparameter analyzer CONSORT 831C. The pH of this reference solution was 6.1.

The titanium samples were cut into 1 cm^2 size and brass nut was attached to each experiments using conductive paint to ensure electrical conductivity. The assembly was then embedded into an epoxy resin disk. Then the samples were ground with SiC abrasive paper up to 1000 grit, final polishing was done with 1 μm alumina suspension.

The samples were degreased with ethyl alcohol followed by ultrasonic cleaning with deionised water and dried under a hot air stream.

2.2. Microstructure characterisation

The structural studies were performed with an optical microscope, Olympus PME 3-ADL. The microstructures were revealed by etching in 10%HF + 5%HNO_3 solution for 3-5 s at 25^0C.

2.3. Potentiodynamic polarization studies

For all the electrochemical tests, experiments were performed using an aerated Ringer's solution maintained at 25 ± 1^0C as an electrolyte. The assembled specimen was placed in a glass corrosion cell, which was filled with freshly prepared electrolyte (within 24 hours). A saturated calomel electrode (SCE) was used as the reference electrode and a platinum coil as the counter electrode.

The measurements were performed with a Princeton Applied Research potentiostate (Model 263 A) controlled by a personal computer and a dedicate software (PowerCorr, Princeton Applied Research).

For each specimen, 24 hours of open circuit potential, E_{OC}, measurement was performed initially followed by the linear polarization measurement. Linear polarization was conducted from E_{OC} -150 mV to E_{OC} + 150 mV at a scanning rate of 0.2 mV/s, to identify the b_a (Tafel slopes for the partial anodic processes) and b_c (Tafel slopes for the partial cathodic processes), the i_{corr} (corrosion current density) and the ZCP (zero current potential). It was then followed by the general polarization tests from -600 mV to 1200 mV at a scanning rate of 0.5 mV/s for evaluating the stability of passivation. From the obtained anodic polarization curves, i_{pass} (passivation current density) was determined.

2.4. Electrochemical Impedance Spectroscopy studies (EIS)

The electrochemical impedance spectroscopy (EIS) was performed 24 hours after immersion in aerated solutions at the open circuit potential using a Princeton Applied Research potentiostate (Model 263 A) connected with a Princeton Applied Research 5210 lock-in amplifier.

The spectra were recorded in the 10^{-2} Hz to 10^5 Hz frequency range. The applied alternating potential signal had amplitude of 10 mV.

Table 1. Alloys composition determined by plasma optical emission spectrometry technique

Element	*Al*	*V*	*Zr*	*Fe*	*O_2*	*N_2*	*C*	*Ti*
Ti6Al4V Weight %	5.88	3.91	-	0.021	0.175	0.0153	0.048	balance
Ti6Al4Zr Weight %	6.01	-	4.05	0.032	0.198	0.0184	0.065	balance

Data acquisition and analysis were performed with a personal computer. The spectra were interpreted using the ZSimpWin program. Impedance data were represented in both complex impedance diagram (Nyquist plot) and Bode amplitude and phase angle plots. In the Nyquist graph, the imaginary component of the impedance is plotted as a function of the real component, whereas the Bode representation shows the logarithm of the impedance modulus (Zmod) and phase angle as a function of the logarithm of the frequency. The advantage of the Bode plot is that the data for all measured frequencies are shown and that a wide range of impedance values can be displayed.

Surface morphology after the electrochemical treatments of the samples was studied with a research electronic microscope of Tesla BS 300 type.

3. Results and discussion

3.1. Microstructural characterization

Surfaces of the three alloys exposed at electrochemical testing were characterized from the structural point of view. Both the samples exhibit a biphasic (α-β) microstructure, but with different morphology. The Ti6Al4V alloy has a Widmanstätten-type structure that consists of α-phase lamellae. The optical images from Fig. 1A show basket weave morphology of α-phase regardless of chemical compositions of titanium alloy. The Ti6Al4Zr alloy has an isotropic structure.

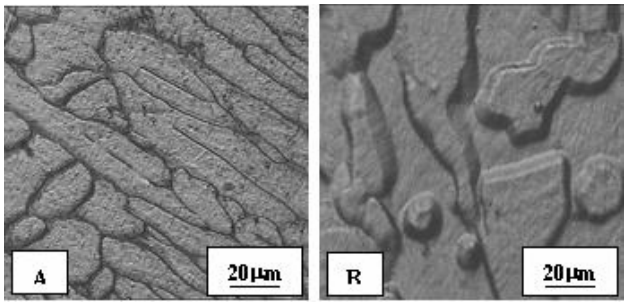

Fig. 1. Micrographs for: (A) Ti6Al4V and (B) Ti6Al4Zr alloys

3.2. Potentiodynamic polarization studies

Fig. 2 shows the E_{OC} curves for both stationary samples immersed in Ringer's solution at 25^0C. The potential pattern with respect to time was similar for both alloys. Initially, the potential of the two titanium based alloys presents approximately the same value: -511 mV for Ti6Al4V and -521 mV for Ti6Al4Zr.

During the first moments of immersion, an abrupt E_{OC} displacement towards positive potentials was noticed in Fig. 2. This initial increase seems to be related to the formation and thickening of the oxide film on the metallic surface, improving its corrosion protection ability (Kedici et al., 1998). Afterwards, the E_{OC} increases slowly suggesting the growth of the film onto the metallic surface. However, Ti6Al4Zr alloy showed nobler potential than Ti6Al4V alloy.

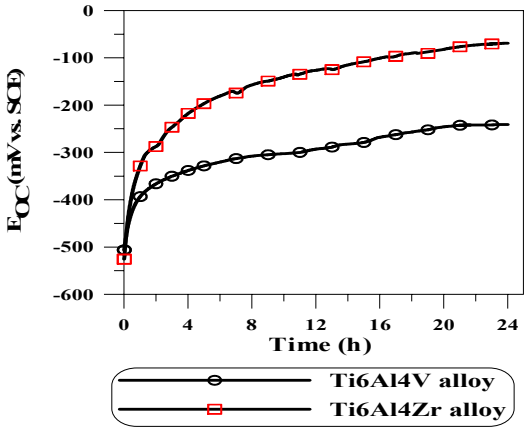

Fig. 2. Variation of open circuit potential (E_{OC}) with time for Ti6Al4V and Ti6Al4Zr alloys in Ringer's type solution

Standard techniques were used to extract zero current potential (ZCP) and corrosion current density (i_{corr}) values from the potentiodynamic polarization plots. The Tafel slopes (b_a and b_c) were determined by fitting the theoretical polarisation curve to the experimental polarisation curve plotted in a range of ± 150 mV vs. E_{OC}. The two Tafel slopes intercept at the point of the coordinates (ZCP, i_{corr}). In most of the aerated neutral solutions the corrosion rate is controlled by the oxygen diffusion at the surface of the electrode when $b_c >> b_a$. This supposition is confirmed by the values presented in the Table 2. The corrosion current density (i_{corr}) is representative for the degradation degree of the alloy. The average values b_a, b_c, ZCP and i_{corr} from polarization curves determined by the PowerCorr program are presented in Table 2. The very low i_{corr} values obtained for both tested titanium alloys are typical of passive materials.

The corrosion current densities for both alloys were of the same order of magnitude (nA/cm^2): 210 nA/cm^2 for Ti6Al4V alloy and 195 nA/cm^2 for Ti6Al4Zr alloy.

Fig. 3 compares typical potentiodynamic curves in a semi-logarithmic version between -600 mV and +1200 mV of the titanium alloys tested in Ringer's solution aerated at 25ºC after being immersed for 24 hours.

The nature of the potentiodynamic polarization curves indicated that Ti6Al4V and Ti6Al4Zr alloys have been passivated immediately after the immersion in the Ringer's solution; both materials translated directly from the "Tafel region" into a stable passive state, without exhibiting a common active-passive transition.

For the potentials above approximately 100 mV up to approximately 300 mV both anodic curves indicates behaviour typical of activation polarization showing a well defined linear range, suggesting conformity to the Tafel's Law.

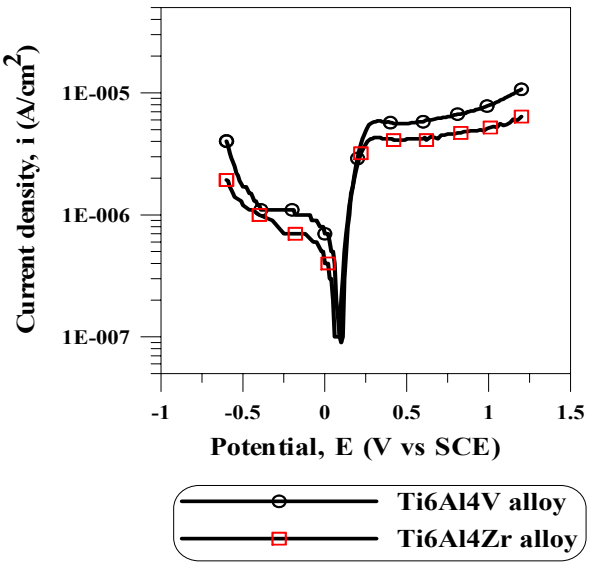

Fig. 3. The potentiodynamic polarisation curves for titanium alloys after 24 hours of immersion in Ringer's type solution

From 300 mV the curves show a passive behaviour. Passive current density (i_{pass}) was also determined from the potentiodynamic anodic diagram of each specimen in Ringer's solution. Passive current densities (i_{pass}) are obtained around the middle of the passive range and are listed in Table 2.

The passive current densities (i_{pass}) for both alloy samples are higher than corrosion current densities (i_{corr}) and suggest that the protective Ti oxide film can be more defective (Lavos-Valereto et al., 2004; Assis et al., 2006; Cremasco et al., 2008). From the polarization curves it was found that both alloys are maintained in their passive state at 1.2 V potential too. No breakdown was observed for Ti6Al4V and Ti6Al4Zr alloys.

No significant differences were found in ZCP, i_{corr} or i_{pass} for both the samples. The results indicate that the polarization curves behaviour of the Ti6Al4Zr alloy resembles that of the Ti6Al4V alloy. Ti6Al4Zr alloy had a good corrosion resistance within the potential range used in this study.

Fig. 4 shows the SEM image of Ti6Al4V alloy after the electrochemical treatments. After electrochemical treatments salt depositions were formed on the surface of the alloy.

The Ringer's solution contains calcium ion, which generally precipitates on titanium alloys surface.

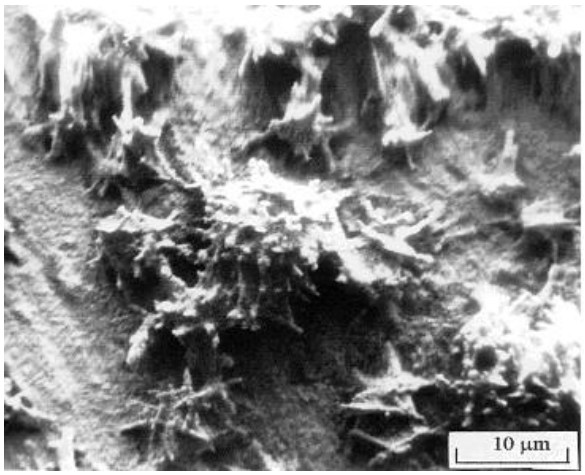

Fig. 4. The salts depositions on the surfaces of the Ti6Al4V alloy

3.3. Electrochemical impedance spectroscopy (EIS) studies

The corrosion resistance can also be estimated by means of the impedance method known as Electrochemical Impedance Spectroscopy (EIS). This technique requires minimal invasive procedures, neither the oxidation nor the reduction was forced to take place in the open circuit mode.

Fig. 5 showed the EIS data, in the form of Nyquist plot, of Ti6Al4V and Ti6Al4Zr alloys at open circuit potential, after 24 hours of immersion in Ringer's solution.

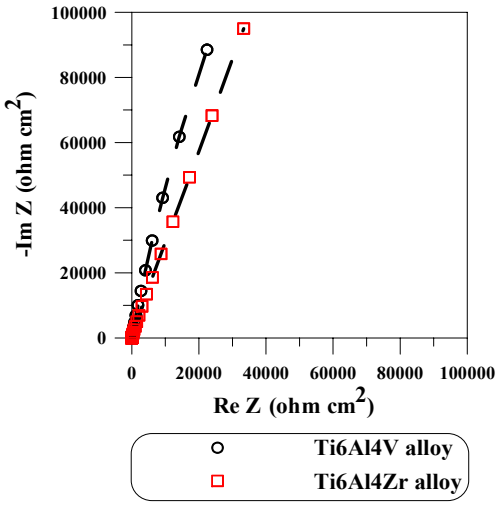

Fig. 5. Nyquist plots of Ti6Al4V and Ti6Al4Zr alloys at open circuit potential, after 24 hours immersion in Ringer´s solution

Table 2. The main parameters of corrosion process after 24 h of immersion in Ringer's type solution

Alloy	*ZCP (mV)*	*b_a(mV dec.$^{-1}$)*	*b_c(mV dec.$^{-1}$)*	*i_{corr} (nA cm^{-2})*	*i_{pass}(μA cm^{-2})*
Ti6Al4V	88	85	∞	210	6.1
Ti6Al4Zr	96	82	∞	195	4.8

Both diagrams show a capacitive arc. The capacitive arc may be related with the dielectric properties of the formed film on the electrode surface at the open circuit potential but it may be also related to the electric double-layer capacitance at the electrode/solution interface, which includes a metal-film interface followed by a film-solution interface.

In the Fig. 6 for titanium alloys the EIS spectra are shown in Bode plots of the logarithm of impedance magnitude and of the phase angle as a function of the frequency's logarithm.

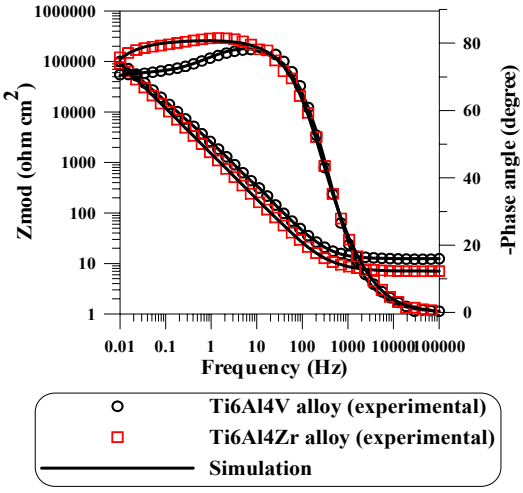

Fig. 6. Bode plots of tested materials recorded at open circuit potential after immersion for 24 hours in Ringer´s type solution

A capacitive behaviour, typical of passive materials is indicated from medium to low frequencies range by phase angle approaching -80^0, suggesting that a stable film is formed on both tested alloys in the electrolyte used. The large phase angle peak could be indicative of the interaction of at least two time constants.

For the interpretation of the electrochemical behaviour of a system from EIS spectra, an appropriate physical model of the electrochemical reactions occurring on the electrodes is necessary. The electrochemical cell may be representing by an equivalent circuit (EC).

The impedance results were interpreted using the ZSimpWin software. After testing a number of different electrical circuit models in the analysis of the impedance spectra obtained at the open circuit potential, it was found that the whole set of data for both the samples could be satisfactorily fitted with the EC given in Fig. 7. This is based on the consideration of a two-layer model for the surface film. The results of the analysis are shown in Table 3.

In Fig. 6 the experimental data are shown by the symbols and the simulated data, which are generated using the equivalent circuit depicted in Fig. 7, are shown as the solid lines.

The Ringer solution contains calcium ion, which generally precipitates on titanium surface form a layer. The high-frequency parameters R_1 and Q_1 represent the properties of the reactions at the outer precipitate layer/solution interface. The symbol Q signifies the possibility of a non-ideal capacitance (CPE, constant phase element). The impedance of the CPE is given by (Raistrick et al., 1987):

$$Q = Z_{CPE} = \frac{1}{C(j\omega)^n} \qquad (1)$$

where for n = 1, the Q element reduces to a capacitor with a capacitance C and, for n = 0, to a simple resistor. The parameter R_2 coupled with Q_2 describes the processes at the inner barrier layer at the electrolyte/passive film interface.

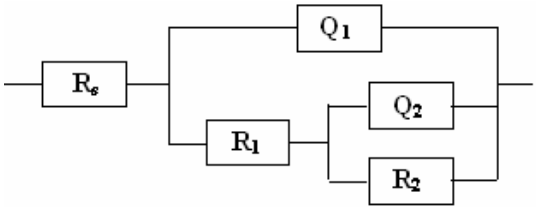

Fig. 7. Equivalent circuit (EC) used in the generation of simulated data

The EIS results exhibited capacitive behaviour (high corrosion resistance) with phase angle close to -80^0 and large impedance values (order of 10^5 Ω cm^2) at medium and low frequencies, which are indicative of the formation of a stable film on these materials in the Ringer's solution.

The same value for R_s, equals 35Ω, was observed for both specimens after 24 hours of immersion and was not inserted in Table 3.

Polarization resistance (R_p) is represented by the sum of the resistance of the inner and outer layer, $R_1 + R_2$. A high R_p value is an indication of the working electrode strongly resisting change from its equilibrium state and corresponds to a low rate of titanium ion release. From the Stern-Geary equation (Stern and Geary, 1957):

$$i_{corr} = \frac{b_a b_c}{2.3R_p(b_a + b_c)} = \frac{B}{R_p} \qquad (2)$$

where: b_a and b_c are the Tafel slopes for the partial anodic and cathodic processes, respectively and B is a constant:

$$B = \frac{b_a b_c}{2.3(b_a + b_c)} \qquad (3)$$

The polarization resistance of the alloys after 24 hours of immersion is large indicating a sufficient stability of titanium alloys in Ringer's solution. The corrosion currents for both titanium alloys were of the same order of magnitude (nA/cm^2) and are in agreement with the polarization data.

Table 3. The main parameters of the proposed equivalent circuit obtained for both studied samples

Alloy	R_1 (Ω cm^2)	n_1	Q_1 (S s^n cm^{-2})	R_2 (Ω cm^2)	n_2	Q_2 (S s^n cm^{-2})	i_{corr} (nA cm^{-2})
Ti6Al4V	1.1 10^3	0.75	2.6 10^{-5}	2.1 10^5	0.87	4.6 10^{-5}	175
Ti6Al4Zr	1.7 10^3	0.76	2.2 10^{-5}	2.3 10^5	0.88	2.7 10^{-5}	161

The exponents of the Q_1, n_1, are equals a value in between 0.75 and 0.76 while the exponents of the Q_2, n_2, are equals a value in between 0.87 and 0.88. This indicates that Q_2 corresponds to a capacitance of the inner layer while, Q_1 is a consequence of frequency dispersion of the outer layer (Tkalcec, 2001).

Results indicate that the electrochemical behaviour of the Ti6Al4Zr alloy examined resembles that of the Ti6Al4V.

4. Conclusions

The electrochemical techniques used in this investigation led to the following conclusions:

a) Ti6Al4V and Ti6Al4Zr alloys exhibited stable passive polarization behaviour. Very low corrosion current densities were obtained for both titanium alloys tested in Ringer's solution. The passivation behaviour of Ti6Al4Zr was comparable with that of Ti6Al4V.

b) The EIS spectra results indicated that the film formed on the titanium materials is composed of a bi-layered consisting of an inner barrier layer associated to high impedance and responsible for corrosion protection and an outer precipitate layer.

c) Both electrochemical techniques show that Ti6Al4Zr alloy exhibits corrosion behaviour in Ringer's solution similar to Ti6Al4V alloy in the as-received condition. The electrochemical and corrosion behaviour of Ti6Al4V is not affected on substituting vanadium with zirconium.

Note

This paper is especially dedicated to Professor Neculai Aelenei on his 70th anniversary.

References

Assis S.L., Wolynec S., Costa I., (2006), Corrosion characterization of titanium alloys by electrochemical techniques, *Electrochim. Acta*, **51**, 1815-1819.

Boyer H.E., Gall T.L., (1985), *Metals Handbook*, ASM International, USA.

Cremasco A., Osorio W.R., Freire C.M.A., Garcia A., Caram R., (2008), Electrochemical corrosion behavior of a Ti-35Nb alloy for medical prostheses, *Electrochim. Acta*, **53**, 4867-4874.

Collings E.W., (1984), *The Physical Metallurgy of Titanium Alloys*, ASM International, USA.

Donachie M.J., (1988), *Titanium -A Technical Guide*, ASM International, USA.

Eriksson C., Ohlson K., Richter K., Billerdahl N., Johansson M., Nygren H., (2007), Callus formation and remodelling at titanium implants, *J. Biomed. Mater. Res.*, **83A,** 1062-1069.

Gonzalez J.E.G., Mirza Rosca J. C., (1999), Study of the corrosion behaviour of titanium and some of its alloys for biomedical and dental implant applications, *J. Electroanal. Chem.*, **471**, 109-115.

Hallab N.J., Anderson S., Caicedo M., Brasher A., Mikecz K., Jacobs J. J., (2005), Effects of soluble metals on human peri-implant cells, *J. Biomed. Mater. Res.*, **74A**, 124-140.

Kedici S.P., Aksut A.A., Kilicarslan M.A., Bayramoglu G., Gokdemir K., (1998), Corrosion behaviour of dental metals and alloys in different media, *J. Oral Rehabil.*, **25**, 800-808.

Khan M. A., Williams R. F., Williams D. F., (1996), In-vitro corrosion and wear of titanium alloys in the biological environment, *Biomaterials*, **17**, 2117-2126.

Kim H. S., Lim S. H., Yeo I. D., Kim W. Y., (2007), Stress-induced martensitic transformation of metastable β-titanium alloy, *Mater. Sci. Eng.,* **449A**, 322-325.

Kuphasuk C., Oshida Y., Andres C. J., Hovijitra S.T., Barco M.T., Brown D. T., (2001), Electrochemical corrosion of titanium and titanium-based alloys, *J. Prosthet. Dent.*, **85**, 195-202.

Lavos-Valereto I.C., Wolynec S., Ramirez I., Gustaldi A. C., Costa I., (2004), Electrochemical impedance spectroscopy characterization of passive film formed on implant Ti6Al7Nb alloy in Hank's solution, *J. Mater. Sci: Mater. Med.*, **15**, 55-59.

Mantani Y., Tajima M., (2006), Effect of ageing on internal friction and elastic modulus of Ti–Nb alloys, *Mater. Sci. Eng.*, **442A**, 409-413.

Mirza Rosca J.C., Vasilescu E., Mareci D., Ivănescu S., Santana López A., (2008), Structural characteristics and anticorrosive properties of a Titanium alloy, *Rev. Chim.*, **59**, 331-335.

Newman J. R., Eylon D., Thorne J. K., (1988), *Titanium and Titanium Alloys, Metals Handbook,* ASM International, Metals Park, Ohio, USA.

Okazaki Y., Rao S., Ito Y., Tateisji T., (1998), Corrosion resistance, mechanical properties, corrosion fatigue strength and cytocompatibility of new Ti alloys without Al and V, *Biomaterials*, **19**, 1197-1215.

Popa M. V., Demetrescu I., Vasilescu E., Drob P., Santana López A., Mirza Rosca J. C., Vasilescu C., Ionita D., (2004), Corrosion susceptibility of implant materials Ti–5Al–4V and Ti–6Al–4Fe in artificial extra-cellular fluids, *Electrochim. Acta*, **49**, 2113-2121.

Raistrick I. D., MacDonald J. R., Francschetti D. R., in: J.R. MacDonald (Ed.), (1987) *Impedance Spectroscopy Emphasizing Solid Materials and Systems*, John Wiley&Sons, New York, USA.

Stern M., Geary A., (1957), Electrochemical polarization I: theoretical analysis of shape of polarization curves, *J. Electroch. Soc.*, **104**, 56-63.

Taddei E.B., Henriques V.A.R., Silva C.R.M., Cairo C.A. A., (2004), Production of new titanium alloy for orthopaedic implants, *Mater. Sci. Eng.*, **24C,** 683-687.

Tkalcec M., Sauer M., Nonninger R., Schmidt H., (2001), Sol-gel-derived hydroxyapatite powders and coatings, *J. Mater. Sci.*, **36**, 5253-5263.